# Articles

## Conformational Analysis of the Prototype Nonclassical Cannabinoid CP-47,497, Using 2D NMR and Computer Molecular Modeling

Xiang-Qun Xie,[†,§] De-Ping Yang,[†,§] Lawrence S. Melvin,[‡] and Alexandros Makriyannis*[,†,§]

*Section of Medicinal Chemistry and Pharmacognosy, School of Pharmacy, The University of Connecticut, Storrs, Connecticut 06269, The Francis Bitter National Magnet Laboratory, Massachusetts Institute of Technology, Cambridge, Massachusetts 02139, and Central Research, Pfizer Inc., Groton, Connecticut 06340*

*Received December 10, 1993*[•]

In an effort to determine the stereochemical requirements for pharmacological activity among the series of nonclassical cannabinoids synthesized at Pfizer, we have studied the conformational properties of the parent bicyclic analog CP-47,497. For this study, we have used a combination of solution NMR and theoretical computational approaches. The energetically favored conformation has the phenolic ring almost perpendicular to the cyclohexanol ring which exists in a chair conformation. The OH bond of the phenol is preferentially coplanar with the aromatic ring and points toward the C2 ring proton, while the dimethylheptyl side chain adopts a conformation almost perpendicular to the aromatic ring. The conformational features of this nonclassical cannabinoid analog closely resemble those of its classical counterparts. The only apparent difference is the small dihedral angle ($\varphi_1$ = 62°) between the planes of the two rings of CP-47,497 compared to that of the tricyclic tetrahydro- or hexahydrocannabinol analogs ($\varphi_1$ = 137°). However, CP-47,497 can be perfectly superimposed over the respective tricyclic analog by rotation around the Ph–cyclohexyl bond (C6–C7 bond) and assume a conformation which is energetically higher than the preferred one by 3.0 kcal/mol. It can be argued that such a conformation may be acquired by the nonclassical analog during its interaction with the active site.

### Introduction

Cannabinoids are molecules related structurally to (–)-$\Delta^9$-tetrahydrocannabinol ($\Delta^9$-THC), the psychoactive constituent in marijuana.[1] Preparations of *Cannabis sativa* (e.g., marijuana, hashish, bhang) were used for therapeutics and recreation as early as 3000 B.C. Currently, potential therapeutic applications include analgesia, sedation, attenuation of the nausea and vomiting due to cancer chemotherapy, appetite stimulation, decreasing bronchial constriction, decreasing intraocular pressure in glaucoma, and treatment of certain motor or convulsant disorders.[1,2] Although the pharmacological properties and structure–activity relationships of cannabinoids are well documented,[3,4] the molecular mechanism of action of these drugs remains unknown. Efforts to understand how these drugs work at the molecular level have been aided by the recent identification and cloning of the brain cannabinoid receptor,[3,5] and especially by the latest characterization of a peripheral receptor for cannabinoids.[6] There are also extensive data indicating that some of the pharmacological properties of cannabinoids may be correlated with their effects on cellular membranes.[4] Existing evidence indicates that molecular geometry plays an important role in determining the activity of these molecules and that both the cannabinoid–membrane interactions and the receptor-mediated effects can be correlated with the stereoelectronic properties of these molecules.[4]

While searching for novel pharmacologically selective analogs possessing analgesic properties but devoid of the undesirable psychotropic properties of $\Delta^9$-THC,[7] researchers at Pfizer synthesized a series of analogs corresponding to the target molecule with the minimum structural features required for analgesia.[8] Those analogs were named *nonclassical cannabinoids* (NCCs) since they deviate structurally from the naturally occurring tricyclic tetrahydrocannabinol by the absence of a tetrahydropyran ring.[7,9] However, only limited data dealing with conformational preferences of these molecules are available.[8] We have been interested in studying conformational properties of the nonclassical cannabinoids for correlation with biological activity.

In the present paper, we investigate the prototype nonclassical cannabinoid CP-47,497, which incorporates the minimal structural requirements for cannabinoid activity and is approximately 10 times more potent than the naturally occurring (–)-$\Delta^9$-THC. The complete chemical shifts of CP-47,497 were assigned from one- and two-dimensional (1D and 2D) NMR experiments. The conformational analysis of CP-47,497 required a careful interpretation of NOE cross-peaks in terms of dipole–dipole interactions as well as the determination of interproton dihedral angles calculated from $^1$H–$^1$H vicinal coupling constants. The preferred orientations of the phenolic OH and dimethylheptyl (DMH) side chain, as well as the preferred relative orientation of the A- and C-rings, were determined from NOEs obtained by analysis of the 2D NOESYPH spectrum. The Karplus relationship was used to estimate dihedral angles from $^1$H–$^1$H vicinal coupling constants with the aid of spectral simulations using the PANIC program; this information was used to define the conformation of the cyclohexyl ring. All NMR results were confirmed by theoretical computational studies. The preferred molecular conformation was then

* Send correspondence to Dr. A. Makriyannis, School of Pharmacy, U-92, The University of Connecticut, Storrs, CT 06269-2092.
† The University of Connecticut.
‡ Pfizer Inc.
§ Massachusetts Institute of Technology.
• Abstract published in *Advance ACS Abstracts*, April 1, 1994.

0022-2623/94/1837-1418$04.50/0 

determined by maximal agreement between the NMR analysis and the computer modeling study. Although our experimental data point to a single preferred conformation for the cyclohexane ring, the results do not exclude the possibility of some averaging between several almost equivalent chair conformations. Conversely, the conformational preference of the side chain involves the averaging of several almost equienergetic conformers. The study concludes with a stereochemical comparison between CP-47,497 and a classical cannabinoid prototype, (−)-9-nor-9β-hydroxy(dimethylheptyl)hexahydrocannabinol (HHC-DMH).

## Experimental Section

**Materials.** Nonclassical cannabinoids were kindly provided to us by Pfizer Central Research (Groton, CT). Deuterated chloroform ($CDCl_3$) and tetramethylsilane (TMS) were purchased from Aldrich Chemical Co. (Milwaukee, WI). NMR samples were prepared as 0.02 M in $CDCl_3$ for $^1H$ NMR and 0.2 M for $^{13}C$ NMR, thoroughly degassed, and sealed in high quality 5-mm NMR tubes (No. 528, Wilmad Glass Co., Buena, NJ). TMS was used as an internal chemical shift reference in all samples.

**NMR Spectroscopy.** The high-resolution 1D and 2D NMR spectra were obtained on Bruker AC-300 and WP-200SY spectrometers. All are equipped with variable temperature probes and adequate software to perform 2D experiments and spectral simulations. All data were collected using pulse sequences and phase-cycling routines provided in the Bruker or other compatible library of pulse programs. Data processing, including sine-bell apodization, Fourier transformation, symmetrization, and plotting, were performed using Bruker's software packages. 1D 300-MHz $^1H$ NMR spectra were recorded using the acquisition parameters: pulse width, 7.0 μs (45° tip angle); spectral width, 3496.5 Hz (11.6 ppm); data size, 64 K (0.11 Hz/point); recycling delay, 5 s; number of transients, 128; temperature, 295 K. The 75-MHz $^{13}C$ DEPT spectra[10] were performed using a 5-mm $^1H/^{13}C$ dual probe with 90° pulses of 10.6 μs for $^1H$ and 6.1 μs for $^{13}C$; spectral width, 18518.5 Hz (247 ppm); data size, 64 K (0.56 Hz/point); recycling delay, 3 s; number of transients, 4096; temperature, 300 K. 2D $^1H$–$^1H$ correlation COSY spectra[11] were recorded at 300 MHz using the acquisition parameters: recycling delay (D1), 2 s; D0 increment, 424 μs; spectral width in F2, 2358 Hz, and in F1, 1179 Hz; temperature, 295 K. The data sizes were 512w in F1 and 1K in F2, and the data were zero-filled in F1 prior to 2D Fourier transformation to yield a 1K × 1K data matrix. The spectra were processed using a sine-bell window function in F1 and F2 (WDW = s), and the data were symmetrized about the diagonal (SYM). The spectra were presented in the absolute value mode (MC2 = M). Resolution in both frequency dimensions was 4.6 Hz/point for each D0. 2D $^1H$–$^{13}C$ heteronuclear correlation (hetero-COSY) experiments were performed at 75 MHz using the parameters: relaxation delay D1, 2s; initial D0 value, 3 μs; fixed mixing period delay D3 and D4, 3.45 and 1.72 ms; spectral width in F1 and F2, 9433.96 Hz (250 ppm) and 1091.70 Hz (7.3 ppm); size in F2, 4K; size in F1, 512w; window function in F2, shift sine bell (SSB = 10), and in F1, Gaussian bell (GB = 0); dummy scans, 4; number of acquisitions, 512; number of experiments, 128. 2D phase-sensitive $^1H$–$^1H$ nuclear Overhauser enhancement (NOESYPH) spectra[13] were recorded at 200 MHz using the acquisition parameters: recycling delay (D1), 2 s; initial delay D0 value, 3 μs; spectral width in F1 and F2, 1562.5 and 781.2 Hz. The mixing time D9 for the NOESYPH experiment was 700 ms. The data sizes were 256w in F1 and 1K in F2, and the data were zero-filled in F1 before Fourier transformation to yield a 1K × 1K data matrix. The data were processed using a sine-bell window function in F1 and F2 (SSB2 = 3, SSB1 = 2).

1D $^1H$ NMR spectral simulations were performed using Bruker's LAOCOON-based PANIC software[14] and as we have described elsewhere.[15] The computer program accepts a maximum of nine nuclear spins of magnetically equivalent groups and requires input of coupling constants and chemical shifts. Line width, spectral width, and data size are adjustable parameters. The spectral parameters defining the spin systems comprise chemical shifts and scalar coupling constants ($J$ coupling) which were measured or estimated from 2D phase-sensitive COSY spectra. These values were used as the starting point for an iterative simulation of subspectra. The refined $^3J$ values were then used to calculate the dihedral angles from the Karplus equation as described later.

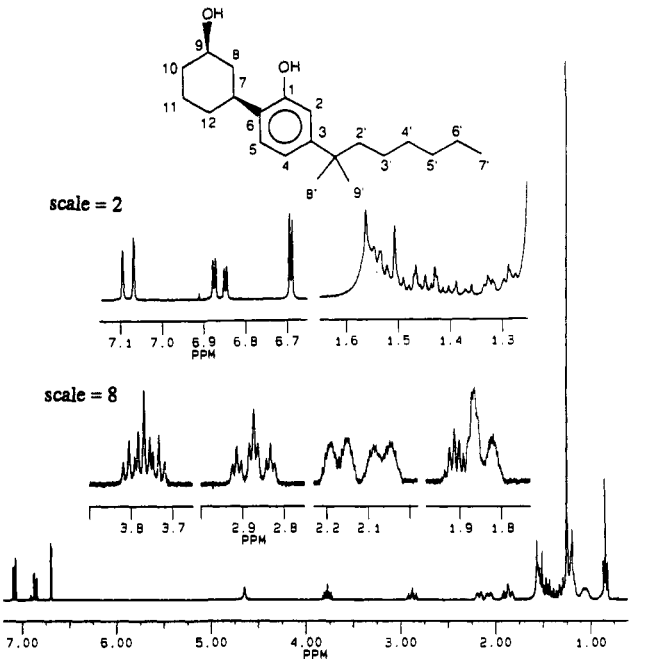


**Figure 1.** 300-MHz $^1H$ NMR spectrum of CP-47,497 in $CDCl_3$ at 295 K in full and expanded scales.

**Computer Molecular Modeling.** Molecular modeling was carried out with the Biosym InsightII/DISCOVER molecular modeling package incorporating an empirical force field, the consistent valence force field (CVFF),[16] on an Iris Silicon Graphics 4D/70GT workstation. Molecular mechanics and dynamics were utilized to investigate the minimum-energy conformations. Bond-rotary searches were used to calculate rotational energy barriers.[17] Molecular dynamics simulations were performed at 1000 K and time steps of 1 fs to search through the different conformations visited during the dynamics simulation.[18] The method involved the following three steps: (1) minimizing the initial structure to relieve any overly strained coordinates using a minimization of steepest descent method for 100 cycles until the maximum derivative was less than 0.1 kcal mol$^{-1}$Å$^{-1}$; (2) performing molecular dynamics sampling of conformational space using the following protocol with time steps of 1 fs, (i) heating up to a certain high temperature and equilibrating at the given temperature (1000 K) for 1 ps and (ii) simulating at this temperature for 300 ps with atomic coordinate trajectories recorded every 1 ps; and (3) retrieving the 300 frames recorded as a *history* file during the dynamics run and minimizing them as an *archive* file with a two-step minimization, steepest descent method for the first 100 iterations and then a conjugate gradient method until the maximum derivative was less than 0.001 kcal mol$^{-1}$Å$^{-1}$. Rotary searches (or dihedral drive technique) were also carried out to calculate energy barriers. Normally, typical intervals of 5° were used for single-bond rotation and 10° for two-bond rotation. However, the energy barriers calculated by simply rotating about a bond while maintaining the other rigid bonds and angles could be misleading and sometimes gave a very high barrier due to van der Waals overlapping. To avoid this problem, an additional torsion force (400 kcal/rad$^2$) was applied to restrain the dihedral angle at the new value to which it was rotated and then followed by energy minimization without cross terms and morse potential (for CVFF). This process was used to relax the entire molecule.

## NMR Results

**Chemical Shift Assignments.** The 300-MHz $^1H$ NMR spectrum of CP-47,497 is shown in Figure 1. The spectral assignments were made initially by an analysis

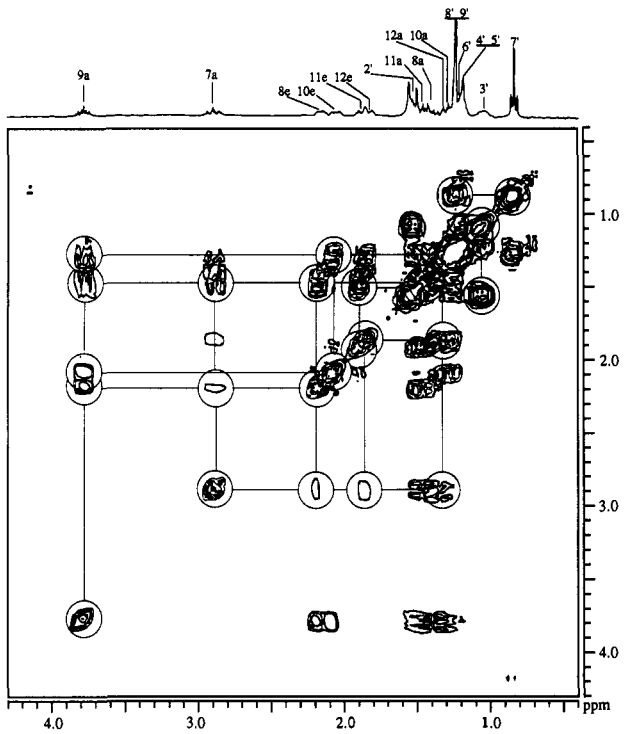


**Figure 2.** Expanded-scale contour plot of a 300-MHz 2D COSY spectrum of the aliphatic resonances of CP-47,497 in $CDCl_3$ solution at 295 K. The coupling networks for the cyclohexane ring and the side chain are highlighted.

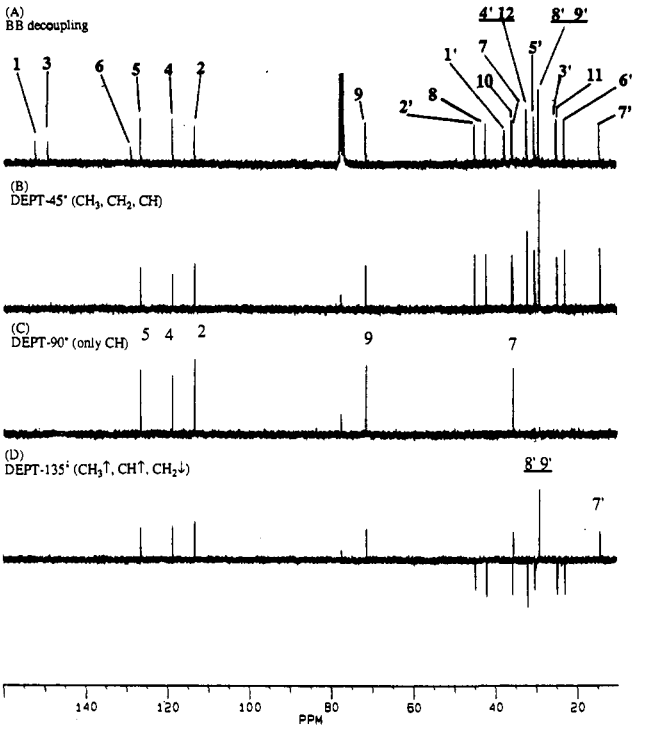


**Figure 3.** 75-MHz $^{13}C$ NMR spectra of CP-47,497 in $CDCl_3$ at 300 K. (A) Normal broad-band decoupled $^{13}C$ spectrum; (B) DEPT 45° spectrum, all of the protonated carbons ($CH_3$, $CH_2$, and CH) appear in this spectrum. (C) DEPT 90° spectrum, only the CH groups appear in this spectrum. (D) DEPT 135° spectrum in which the $CH_3$ and CH carbons appear with positive amplitudes and the $CH_2$ carbons appear with negative amplitudes.

based on chemical shifts. Subsequently, they were specifically assigned on the basis of their coupling connectivities as seen in the $^1H$–$^1H$ homonuclear COSY spectrum and confirmed by DEPT, $^1H$–$^{13}C$ heteronuclear COSY, and phase-sensitive NOESY experiments. The aromatic protons and the aliphatic protons of the 1′,1′-dimethylheptyl side chain were first assigned by analogy with 1-phenylheptane and *tert*-butylbenzene and then confirmed by analyzing the results of the 2D COSY experiment. As shown in Figure 1, the most downfield signals were assigned to the aromatic protons. H-4 and H-5 can be readily distinguished by their $^3J$ cross-peaks in the COSY spectrum (not shown). The side-chain dimethyl resonances (8′ and 9′) were magnetically equivalent and were identified in the spectrum (Figure 1) as the high-intensity broadened singlet integrating for six hydrogens. The side-chain terminal methyl signal (7′) was located further upfield as a triplet integrating for three hydrogens. The 2′-$CH_2$ resonances imbedded among other signals could be identified on the basis of the coupling network in the COSY spectrum (Figure 2) and NOE effects in the NOESYPH spectrum. Noticeably, the $^1H$–$^1H$ COSY spectrum showed that the protons at the 3′-position were shifted upfield to $\delta$ 1.06 ppm. As will be discussed later, this observation served as evidence for the preferred conformation of the dimethylheptyl side chain.

The proton signals belonging to the cyclohexyl ring were assigned on the basis of their connectivities from the coupling cross-peaks in both the 2D homo- and hetero-COSY experiments. A logical point to start the analysis was the most downfield aliphatic proton H-9a which was at $\delta$ 3.77 ppm and integrated for one proton. The axial H-9a was coupled to H-10a, H-8a, H-10e, and H-8e through a vicinal mechanism which we also identified through the cross-peak connectivities in the COSY spectrum (Figure 2). Similarly, the $J$-coupling cross-peak connectivities of H-7a with H-8a, H-12a, H-8e, and H-12e were identified. The axial and equatorial hydrogens of H-8, -10, -11, and -12 were differentiated on the basis of their respective vicinal coupling constants. The axial H-11 could be deduced on the basis of its connectivities with H-10a and H-12a in the COSY spectrum shown in Figure 2.

The above assignments were confirmed by $^{13}C$ DEPT (Figure 3) and $^1H$–$^{13}C$ hetero-COSY (Figure 4). The DEPT method uses the spin–echo technique to edit the $^{13}C$ spectra,[13] i.e., to separate $^{13}C$ spectra into methyl ($CH_3$), methylene ($CH_2$), methine (CH), and quaternary (C) carbons with varied proton polarization pulse angles (P0). In the DEPT 45° experiment, P0 = 5.3 $\mu$s was used to obtain optimal intensities for the protonated carbons, i.e., $CH_3$, $CH_2$, and CH (Figure 3B). By comparing the broad-band decoupled $^{13}C$ spectrum (Figure 3A) with the DEPT 45° spectrum, we could assign the nonprotonated aromatic carbons (C1, C3, and C6) and the C1′ of the side chain (Table 1). The DEPT 90° experiment with P0 = 10.6 $\mu$s identified the CH protons (Figure 3C) and allowed us to assign the signals due to carbons 5, 4, 2, 9, and 7 in the spectrum. The DEPT 135° experiment with P0 = 15.9 $\mu$s gave positive signals for the $CH_2$ and $CH_3$ groups and negative signals for the CH groups (Figure 3D). The $^1H$–$^{13}C$ hetero-COSY gave the proton–carbon connectivities. As shown in Figure 4, the $^{13}C$–$^1H$ COSY spectrum is useful for identification of the *axial* and *equatorial* protons in the cyclohexyl ring. In addition to that, we found that the $^{13}C$ signal of 3′-$CH_2$ is at $\delta$ 24.66 ppm which is upfield relative to other methylene groups. This observation will be discussed later. The two hydroxyl groups were assigned using a 2D exchange experiment. A summary of $^1H$ and $^{13}C$ chemical shifts is given in Table 1.

**Coupling Constant Measurements.** The $^2J$ and $^3J$ values were approximated by first-order analysis of the

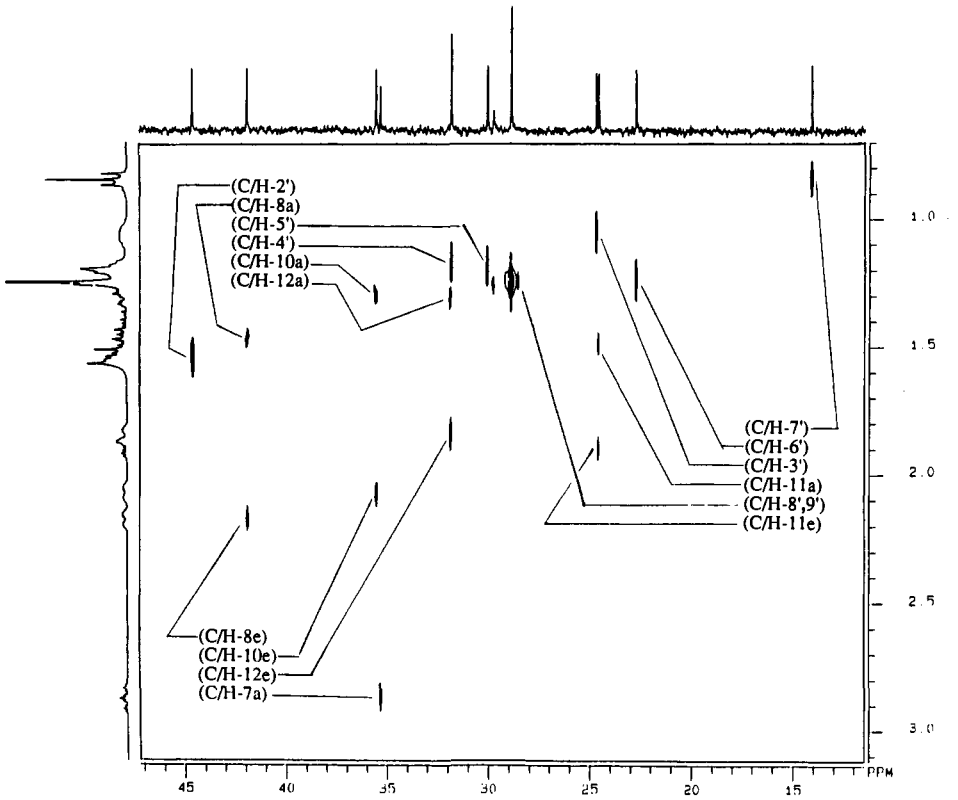


**Figure 4.** Expanded scale of a 300-MHz 2D $^1H$–$^{13}C$ COSY spectrum of CP-47,497 in $CDCl_3$ at 300 K, showing the $^1J_{CH}$ interactions of aliphatic resonances with the $^1H$ spectrum projected in the F1 dimension and the $^{13}C$ spectrum in the F2 dimension.

**Table 1.** $^1H$ NMR (300 MHz) and $^{13}C$ NMR (75 MHz) Chemical Shift Assignments of CP-47,497 in $CDCl_3$ Solution at 295 K, with TMS as Internal Reference

| hydrogen | chemical shift (ppm) | carbon | chemical shift (ppm) |
|---|---|---|---|
| 2 | 6.69 | 1 | 152.22 |
| 4 | 6.86 | 2 | 113.08 |
| 5 | 7.08 | 3 | 149.18 |
| 7 | 2.87 | 4 | 118.54 |
| 8e | 2.17 | 5 | 126.36 |
| 8a | 1.45 | 6 | 128.72 |
| 9a | 3.77 | 7 | 35.28 |
| 10e | 2.07 | 8 | 41.88 |
| 10a | 1.28 | 9 | 71.16 |
| 11e | 1.88 | 10 | 35.51 |
| 11a | 1.48 | 11 | 24.54 |
| 12e | 1.84 | 12 | 31.80 |
| 12a | 1.32 | 1′ | 37.30 |
| 2′ | 1.53 | 2′ | 44.58 |
| 3′ | 1.06 | 3′ | 24.66 |
| 4′,5′ | 1.19–1.25 | 4′ | 31.80 |
| 6′ | 1.24 | 5′ | 30.04 |
| 7′ | 0.84 | 6′ | 22.68 |
| 8′,9′ | 1.24 | 7′ | 14.11 |
| 1-OH | 4.65 | 8′ | 28.87 |
| 9-OH | 1.57 | 9′ | 28.87 |

**Table 2.** $^1H$ NMR Coupling Constants and Calculated Dihedral Angles for CP-47,497

| type of coupling | $^1H$:$^1H$ | coupling constant $^nJ$ value[a] (Hz) | dihedral angle[b] (degrees) |
|---|---|---|---|
| geminal $^2J$ | 8a–8e | −12.5 | c |
| | 10a–10e | −12.5 | c |
| | 11a–11e | −12.8 | c |
| | 12a–12e | −12.3 | c |
| vicinal $^3J$ | 7a–8a | 12.0 | 168 |
| | 7a–8e | 3.1 | 62 |
| | 7a–12a | 12.1 | 170 |
| | 7a–12e | 3.2 | 62 |
| | 8a–9a | 10.9 | 159 |
| | 8e–9a | 4.2 | 57 |
| | 9a–10a | 10.9 | 159 |
| | 9a–10e | 4.2 | 57 |
| | 10a–11a | 11.2 | 161 |
| | 10a–11e | 4.2 | 57 |
| | 10e–11a | 4.2 | 57 |
| | 10e–11e | 2.5 | 64 |

[a] Determined from 1D or 2D experimental spectra and refined through spectral simulation using PANIC. $n$ is the number of bonds through which coupling occurs; geminal, $n = 2$; vicinal, $n = 3$; benzylic or long-range coupling, $n = 4$. [b] Calculated using the equation $^3J = K \cos^2 \phi$, where $K_{a-a} = 12.5$ Hz, $K_{a-e} = K_{e-a} = 14.3$ Hz, and $K_{e-e} = 12.0$ and $\phi$ is the dihedral angle. $K$ values were calculated from 1,3,5-trimethylcyclohexane.[28] [c] Geminal bond angles cannot be quantitatively determined.

individual multiplets obtained as F1 cross-section spectra from the 2D COSY spectrum and 2D $J$-resolved spectrum. These approximated J values and chemical shift values were then used as a starting point for iterative simulation of the subspectra with the help of Bruker's LAOCOON-based PANIC computer program[14] and as we described elsewhere.[15] The iterative simulation process allowed the determination of selected geminal and vicinal coupling constants for the cyclohexyl ring. The coupling constants so determined were then used to calculate the corresponding dihedral angles[14,15,19] (Table 2).

**$^1H$–$^1H$ NOE Measurements.** The three-dimensional relationships between hydrogens were determined by analysis of the NOE cross-peaks, which arise due to dipolar interactions, in the 2D NOESYPH spectrum, since the magnitude of the NOE between two protons depends on the interproton distance ($r^{-6}$).[20] The resulting 2D $^1H$ NOESYPH contour spectrum for CP-47,497 is shown in Figure 5. The molecule under study is of intermediate size and undergoes relatively rapid tumbling with a correlation time, $\tau_c$, of approximately $10^{-10}$ s.[20] For this reason, the NOE buildup rate is correspondingly reduced and the cross-peaks in the NOESY spectrum are of low intensity. This problem was overcome by using a relatively

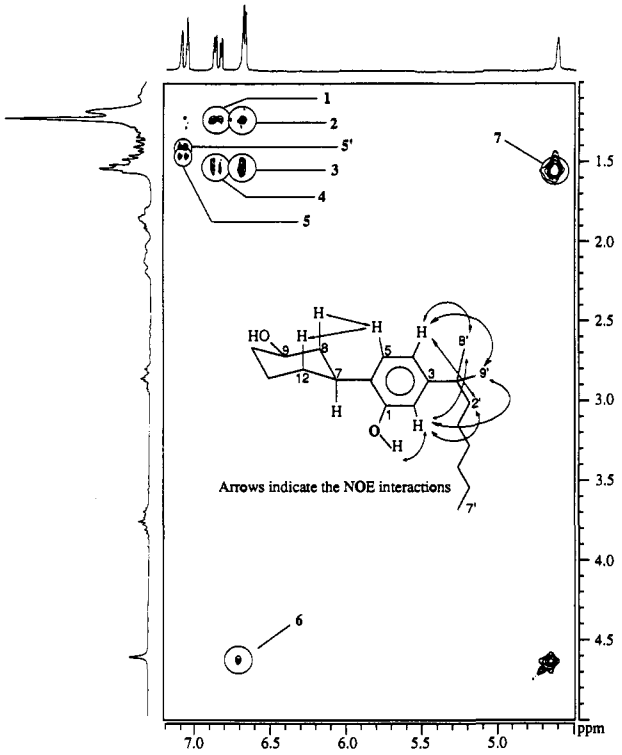


**Figure 5.** Expanded scale of a 200-MHz 2D $^1$H NOESYPH spectrum of CP-47,497 in $CDCl_3$ at 295 K. The experiment was performed in a phase-sensitive (TPPI) mode with variable mixing time, 700 ± 21 ms. The observed NOEs are negative cross-peaks: 1, H-4/H-8′ or -9′; 2, H-2/H-8′ or -9′; 3, H-2/H-2′; 4, H-4/H-2′; 5, H-5/H-8a; 5′, H-5/H-12a; and 6, 1-OH/H-2. The chemical exchange between hydroxyl groups is oberved as a strong positive crosspeak: 7, 1-OH/9-OH. NOE interactions are also represented on the structure of CP-47,497.

long mixing time (700 ms) in order to enhance the NOE effects. To remove possible COSY $J$-coupling cross-peaks due to zero-quantum (ZQ) and double-quantum (DQ) coherence transfer, phase cycling and small (~3%) random fluctuation of mixing times were performed.

A strong NOE cross-peak was observed ($F_1$ = 1.58 ppm, $F_2$ = 4.62 ppm) due to the fast chemical exchange of the two protons between the aliphatic and aromatic OH groups (Figure 5). A relatively weak NOE peak was observed between the phenolic hydroxyl proton ($\delta$ 4.62 ppm) and the aromatic hydrogen (H-2) ($\delta$ 6.65 ppm), indicating that the phenolic hydroxyl proton is pointing away from the cyclohexane ring. This result is similar to those obtained with the classical cannabinoid $\Delta^9$-THC.[15] The spectrum also showed that there are NOE effects between H-5 and H-8a and H-12a but no NOE cross-peaks between H-5 and H-7a. This indicates that H-5 is in proximity with H-8a and H-12a and capable of through-space dipole–dipole coupling but far from H-7a. Information on the conformation of the side chain was obtained on the basis of the observed NOE effects between the aromatic protons H-2 and H-4 and the 2′-, 8′-, and 9′-protons of the DMH side chain. The NOE cross-peaks were observed at $F_1$ = 1.24 ppm, $F_2$ = 6.65 ppm and $F_1$ = 1.24 ppm, $F_2$ = 6.83 ppm, indicating dipolar coupling between the aromatic H-2 and H-4 hydrogens and the 8′- or 9′-geminal methyl groups, respectively. NOE cross-peaks were also observed at $F_1$ = 1.53 ppm, $F_2$ = 6.69 ppm and $F_1$ = 1.53 ppm, $F_2$ = 6.86 ppm, which were attributed to through-space coupling of H-2 with H-2′ and H-4 with H-2′. These NMR interpretations and the conformational depiction of CP-47,497 in Figure 5 were further investigated by computer molecular modeling.

## Molecular Modeling Results

We used computer molecular modeling to probe the conformational features of CP-47,497.[21] A molecular model of $\Delta^9$-THC was initially generated from the X-ray crystallographic data of $\Delta^9$-tetrahydrocannabinolic acid[22] and energy-minimized using the Biosym DISCOVER program.[16] The minimum-energy conformation of $\Delta^9$-THC was then used as a starting template, and the structure of CP-47,497 was generated by deletion and/or addition of atoms at standard bond lengths and bond angles under the Biosym software.

**Molecular Dynamics.** The simulation was carried out in a vacuum condition (default, dielectric constant = 1). A total of 300 000 conformations or frames (1-fs intervals) were sampled during the simulation. In order to reduce the volume of the output data to a more manageable level, conformer structures were recorded at 1-ps intervals, thus reducing the number of structures to be analyzed to 300 frames.

The dynamic behavior of the molecule under study may be best appreciated by following the value of the torsion angles as a function of time during the simulation. The temporal changes of the values of the dihedral angles in various locations in the molecule are given in Figure 6A, thus tracing the history of the dihedral angles $\varphi_1$, $\varphi_2$, $\varphi_3$, and $\varphi_4$ during the dynamics simulation (see Table 3 for the definition of the angles). The torsion angle $\varphi_1$ starts at 60° and increases to more positive values for some 50 ps with some oscillatory motion; then $\varphi_1$ undergoes a sharp transition to near −120°, returns to 60° for about 25 ps, and then returns back to −120° (Figure 6A), and the process is repeated. It appears that the molecule prefers to spend more time at $\varphi_1$ = 60° with the phenolic hydroxyl group pointing down toward the $\alpha$-face of the molecule below the plane of the cyclohexyl ring, rather than at $\varphi_1$ = −120° with the phenolic OH pointing up toward the $\beta$-face. This result is consistent with our NMR data as will be described under Discussion.

While considering the dynamics trajectory during which period the molecule experiences fluctuating conformations, we retrieved six snapshots of instantaneous conformations at various points along the trajectory (Figure 7). As can be seen from these six conformers, conformational variations for CP-47,497 during the molecular dynamics simulation involve mostly changes in the dihedral angle between the two rings as well as in the dihedral angles between the phenolic ring and the dimethylheptyl side chain. The 300 snapshots of random conformations generated during the dynamics simulation were then retrieved and subjected to molecular mechanics manipulation to obtain their minimum-energy conformations. The effect of minimization on these torsion angles is shown in Figure 6B, which outlines the convergence of angles $\varphi_1$, $\varphi_2$, $\varphi_3$, and $\varphi_4$ for CP-47,497.

The convergence resulting from the energy minimization led to eight families of minimum-energy conformations differing from each other by less than 0.9 kcal/mol, a value mainly due to the incomplete minimization of the alkyl side chain. The results of the dynamics and energy minimization calculations are summarized in Table 3.

**Rotational Barriers.** We have also mapped the trajectory of CP-47,497 with regard to torsion potential

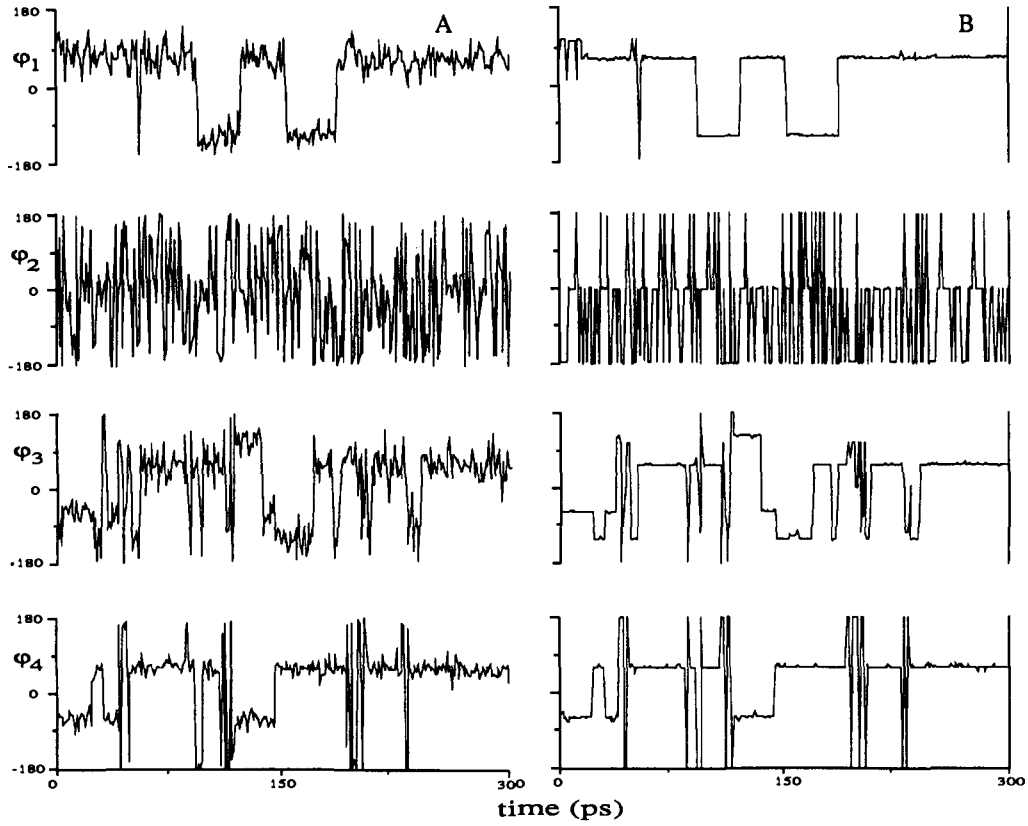


**Figure 6.** (A) History of the torsion angles $\varphi_1$, $\varphi_2$, $\varphi_3$, and $\varphi_4$ as a function of the time elapsed during the molecular dynamics simulations for CP-47,497. (B) Plots of the torsion angles $\varphi_1$, $\varphi_2$, $\varphi_3$, and $\varphi_4$ as functions of the time during the energy minimization of corresponding structures occurring along the molecular dynamics simulations for CP-47,497.

**Table 3.** Preferred Conformations for CP-47,497, Based on Selected Conformers from Molecular Dynamics Simulations which Were Subsequently Minimized

| time (ps) | energy (kcal/mol) | | $(\phi_1, \phi_2, \phi_3, \phi_4)$ (degree)[c] | |
|---|---|---|---|---|
| | dynamics[a] | minimized[b] | dynamics | minimized |
| 5 | 46.7 | 34.0 | (45, 14, -104, 23) | (65, 1.1, -123, 59) |
| 11 | 51.2 | 33.8 | (103, 175, 51, 63) | (64, -178, 55, 58) |
| 169 | 42.1 | 34.4 | (85, -1.9, 143, -68) | (62, -1.5, 122, -60) |
| 180 | 37.3 | 33.9 | (65, -172, -55, 52) | (66, -177, -55, -58) |
| 66 | 58.6 | 34.2 | (123, -94, -154, 58) | (-115, -179, -113, 58) |
| 92 | 46.5 | 33.7 | (-113, -174, 53, -71) | (-116, -178, 56, 59) |
| 200 | 57.2 | 34.3 | (-82, -51, -23, -51) | (-116, 0.5, -54, -59) |
| 292 | 38.7 | 34.6 | (-103, -1.2, 131, -34) | (-116, -1.9, 124, -59) |

[a] The dynamics simulation was performed using CVFF force field with a time step of 1 fs at a temperature of 1000 K for a period of 300 ps. [b] Two steps of energy minimizations (steepest descent and conjugate gradient) were conducted to minimize the 300 frames, which were sampled during the dynamics simulation, until the maximum derivative was less tham 0.001 kcal/mol. [c] $\phi_1$, $\phi_2$, $\phi_3$, and $\phi_4$ are defined as the dihedral angles C5–C6–C7–C8, C2–C1–O–H, C2–C3–C1′–C2′, and C3–C1′–C2′–C3′, respectively.

energy around a single bond using bond-rotary methods for calculating the energy barriers. The rotational energy barriers were calculated by systematically sampling the dihedral angle at intervals of 5° with the angle $\varphi_2$ restrained to −1.5° under a torsion force of 200 kcal/rad$^2$ and followed by energy minimization to relax the entire molecule. The calculated results revealed that the rotational energy barrier for the dihedral angle $\varphi_1$ is 9.7 kcal/mol with the highest energy corresponding to a conformer in which the two rings become coplanar ($\varphi_1$ = 30°) and two minimum points (around 60° and −120°), as indicated in the torsional profile (data not shown). The rotational energy barrier for $\varphi_2$ is low (2.7 kcal/mol), while the rotational energies for $\varphi_3$ and $\varphi_4$ are 7.4 and 8.8 kcal/mol, respectively.

## Discussion

The analysis of our data given below is presented on the basis of the following four features: (i) the conformation of the 1′,1′-dimethylheptyl side chain, (ii) the conformation of the cyclohexyl ring, (iii) the relative orientation of the aromatic (A-ring) and cyclohexyl rings (C-ring), and (iv) the conformation of the phenolic OH group. Our study of the conformational properties of CP-47,497 combines the experimental results determined by solution NMR experiments with computational data obtained from molecular mechanics/dynamics calculations. The preferred conformation is thus determined by maximal agreement between the experimental and computational results. Our approach involves focusing on the conformations of individual molecular components which are subsequently combined to provide a complete picture of the molecule under study.

**Conformation of the 1′,1′-Dimethylheptyl Side Chain.** The conformation of the flexible 1′,1′-dimethylheptyl side chain was analyzed by examining the NOE interactions between the side-chain protons and those of

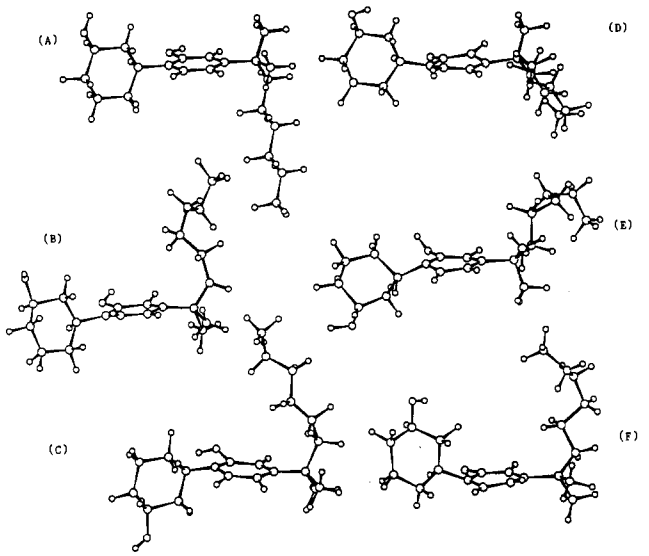


**Figure 7.** Snapshots from molecular dynamics simulations on CP-47,497, employing CVFF at 60-ps time intervals: (A) 1 ps, (B) 60 ps, (C) 120 ps, (D) 180 ps, (E) 240 ps, and (F) 300 ps.

the aromatic ring. The regional expansion of the 2D contour map of the NOESYPH spectrum for CP-47,497 shows NOE interactions (as indicated by arrows in the insert in Figure 5) between the 8′- and 9′-methyl protons ($\delta$ 1.24 ppm) and the aromatic protons H-2 ($\delta$ 6.69 ppm) and H-4 ($\delta$ 6.86 ppm). In addition, nuclear Overhauser effects are also observed between the 2′-$CH_2$ hydrogens ($\delta$ 1.53 ppm) and the H-2 and H-4 aromatic hydrogens. Such NOE cross-peak patterns imply the possibility of several interconverting conformers which are time averaged in the NMR time scale. The NOE data, which are supported by the computational studies, suggest four minimum-energy conformations for the 1′,1′-dimethylheptyl side chain. These include possible $\varphi_3$ values of approximately 60°, −60°, 120°, and −120° obtained through rotation around the C3–C1′ bond and $\varphi_4$ values of 60° and −60° by rotation around the C1′–C2′ bond. Overall, the DMH side chain is almost perpendicular to the plane of phenyl ring and orients with equal probability in one of the above four minimum-energy conformations.

The above finding is further confirmed by the 2D COSY spectrum in which the 3′-$CH_2$ protons have an unusually strong upfield shift (Figure 2). According to chemical shift NMR theory, the 3′-$CH_2$ being in a $\gamma$-position relative to the two methyl groups (8′ and 9′) experiences the $\gamma$-effect and should cause the $^{13}C$ resonance of C3′ to shift upfield due to the steric compression of a gauche interaction accompanied by a shielding of the carbon atom.[23] Conversely, the protons attached to this carbon atom are deshielded and are expected to experience a downfield chemical shift. The $^{13}C$–$^{1}H$ hetero-COSY spectrum (Figure 4) indicates that the C3′ carbon resonance behaves as expected, showing an upfield chemical shift. However, contrary to what was expected by the $\gamma$-effect, the 3′-$CH_2$ protons were found to exhibit an upfield shift ($\delta$ 1.06 ppm). This shielding effect which overcomes the deshielding of the $\gamma$-effect can be attributed to a preferred side-chain conformation in which the 3′-$CH_2$ protons are located above or below the aromatic ring, in agreement with the computational results.

**Relative Orientation between A- and C-Rings.** The NOESYPH spectrum (Figure 5) shows two NOE cross-peaks due to dipolar coupling of H-5 with H-12a and H-5 with H-8a. The contour levels were similar for the two NOE cross-peaks, indicating that H-5 is positioned midway between the two axial protons H-12a and H-8a and thus bisects the C12–C7–C8 angle of the cyclohexane ring. This interpretation is congruent with the molecular mechanics/dynamics results showing that the preferred dihedral angle between the two rings is either ~60° or ~−120° (Table 3). No NOE cross-peak was observed between H-7a and H-5 (Figure 5), thus ruling out a possible conformation in which H-7a and H-5 are pointing in the same direction with $\varphi_1$ ~−120° and the phenolic OH group pointing up. The combined NMR and computational data find a preferred conformation in which the phenolic OH group points down with $\varphi_1$ = 62° and $\varphi_2$ = −1.5°. The above conclusion is congruent with the dynamics simulation data shown in Figure 6A,B which reveal that there were more points around $\varphi_1$ = 60° than −120°. The bond-rotary search for the preferred torsion angle ($\varphi_1$) with the angle $\varphi_2$ restrained to −1.5° (on the basis of the NOE result) also showed that the preferred dihedral angle $\varphi_1$ was 62°, even though the energy difference between $\varphi_1$ = 62° and $\varphi_1$ = −115° is only 0.32 kcal/mol.

Rotation around the C6–C7 bond connecting the two rings revealed two energy minima, separated by a relatively large rotational energy barrier of ~9.7 kcal/mol, the energy being highest when the two rings become coplanar. The data indicate that, in the preferred conformation, the plane of the phenol ring bisects the C12–C7–C8 angle of the cyclohexane ring and the phenolic OH points down ($\varphi_1$ = 62°) and away from the cyclohexane ring ($\varphi_2$ = −1.5°). We were concerned about the relatively high value of the energy barrier around the phenyl–cyclohexyl bonds calculated using Biosym CVFF, especially since this was 3.7 kcal/mol higher than the previously reported values in which MM1 and MM2 calculations were used.[8,29] To place our results in a better perspective and in view of the fact that rotation around the phenyl–cyclohexyl bond represents an important consideration with regard to pharmacophoric requirements for cannabinoid activity, we used two additional methods, namely Tripos Sybyl and MOPAC/AM1. As can be seen from the comparative data listed in Table 4, indeed Biosym seems to overestimate this energy barrier, exceeding the Sybyl and MOPAC results by 3.3 and 4.1 kcal/mol, respectively.

**Table 4.** Comparisons of the Bond Rotational Energies about the Aryl–Cyclohexyl Ring Bond (C6–C7) Obtained Using Different Calculation Methods

| methods | dihedral angle $\phi_1$ minimum | dihedral angle $\phi_1$ maximum | $\Delta E_{max-min}$[c] (kcal/mol) | $\Delta E_{max-137°}$[d] (kcal/mol) |
|---|---|---|---|---|
| Biosym CVFF[a] | 62.0° | −31.3° | 9.7 | 6.1 |
| Tripos Sybyl[b] | 62.1° | −32.2° | 6.4 | 2.7 |
| MOPAC/AM1[b] | 60.2° | −30.3° | 5.6 | 1.9 |

[a] Data were obtained using consistent valence force field (CVFF) under Biosym DISCOVER software on a SGI 4D/70GT workstation. [b] Data were obtained using Tripos force field under Tripos SYBYL software on a SGI Indigo2 workstation. MOPAC/AM1 calculations interfaced under Tripos SYBYL software package were also performed on the Indigo2 workstation. [c] Energy difference between the maximum and global minimum. [d] Energy difference between the maximum and the proposed conformer with the dihedral angle $\phi_1$ = 137° which is superimposable with the pharmacophores of HHC-DMH.

**Conformation of the Phenolic OH.** It is generally accepted that the phenolic OH plays an important role in determining cannabimimetic activity.[4] Consequently, its conformational preference is especially interesting with respect to its interactions at the active site.[4] Existing

data[15,24,25] show that in the biologically active $\Delta^9$-THC, the phenolic OH bond lies in the plane of the aromatic ring and is oriented toward H-2. Our NOE data showing cross-peaks between the Ph–OH and the H-2 proton support a similar conformation for CP-47,497. For our theoretical studies of $\varphi_2$, we used the quantum mechanical semiempirical method MOPAC,[26] which gives more consistent results with conformational studies involving the hydroxyl group. The calculated results with MOPAC (AM1) confirmed our experimental findings and showed that in its preferred conformation the phenolic OH is coplanar with the phenolic ring and points away from the cyclohexyl ring (i.e., $\varphi_2$ near 0°). This conformation is only slightly preferred (by 0.33 kcal/mol) over the corresponding conformers having $\varphi_2 = 180°$.

**Stereochemical Correlation between Classical and Nonclassical Cannabinoids.** To explore the significance of the results from our study with the prototype nonclassical cannabinoid CP-47,497, we have sought to compare its conformational properties to those of a classical cannabinoid prototype which unlike the NCCs has an intact dihydropyran ring. To carry out such a comparison, we have chosen (−)-9-nor-9β-hydroxy(dimethylheptyl)-hexahydrocannabinol.[9] The structural model of HHC-DMH was initially generated and modified on the basis of the X-ray crystallographic data of $\Delta^9$-tetrahydrocannabinolic acid[22] and then energy minimized. This molecule contains the same three key pharmacophores present in CP-47,497, namely a phenolic OH (PH), a side chain on the 3-position of the phenolic ring (SC), and an aliphatic 9β-hydroxyl group in the northern side of the molecule (NAH). A cursory examination of the preferred conformations of the two molecules in question readily reveals that their molecular structures differ in their respective $\varphi_1$ dihedral angles, which describe the relative stereochemical relationship of the phenolic and cyclohexyl rings in each molecule.

In this regard, earlier work from our laboratory,[15,27] which was also confirmed by Reggio and co-workers,[24] suggested that the relative potencies of certain classical cannabinoid analogs could be explained by observed differences in the planarity of these molecules. It was argued that a deviation of 10°–20° in the plane of the ring C within the tricyclic cannabinoid system is a requirement for cannabimimetic activity.

To explore in more detail the similarities and differences in the stereoelectronic properties of these two classical and nonclassical cannabinoid prototypes, we superimposed them on each other (Figure 8). This was accomplished using the bond rotation with the animation technique. We found that optimal superposition is achieved if the $\varphi_1$ dihedral angle of CP-47,497 is changed from its global minimum value of $\varphi_1 = 62°$ to $\varphi_1 = 137°$ by rotation around the C6–C7 bond (structure A′ in Figure 8). In this conformation, the O9–O1 distance is 4.78 Å and the projection angle of the C9–O9 bond on the plane of the aromatic ring determined by measuring the dihedral angle O9–C9–C1–O1 is −50.1°. This compares favorably with the respective values of 4.99 Å and −55.5° in HHC-DMH. Our calculations show that the conformational realignment described above for the two rings of CP-47,497 would require an amount of energy ranging between 1.9 and 6.1 kcal/mol, depending on the method used (Table 4). We

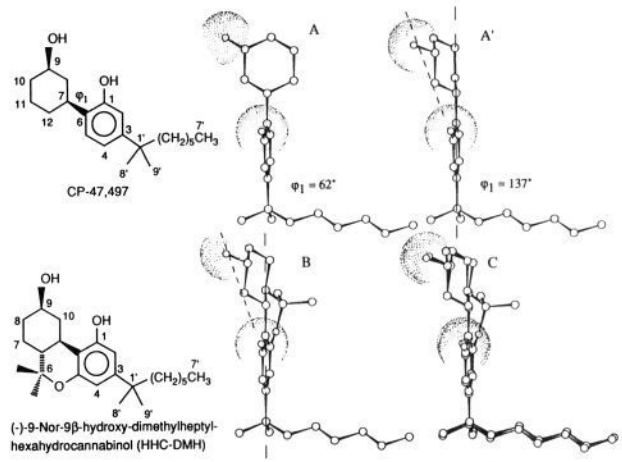


**Figure 8.** Graphic representation of the stereochemical correlation of CP-47,497 with HHC-DMH using a superimposition method. The preferred conformer (A) of CP-47,497 ($\varphi_1 = 62°$, $\varphi_2 = -1.5°$, $\varphi_3 = 122°$, and $\varphi_4 = -60°$) was allowed to rotate to a conformation in which $\varphi_1 = 137°$ (A′). This conformational change requires the expenditure of 6.1 kcal/mol. In this conformation, CP-47,497 is superimposable with the ring systems of the classical cannabinoid HHC-DMH (B). The superimposed structures of CP-47,497 and HHC-DMH are displayed (C).

tend to favor the lower values since Biosym CVFF is known to overestimate energy barriers in small or medium-sized molecules.

On the basis of the above comparisons, it can be argued that CP-47,497 can interact with the cannabinoid receptor in a similar fashion as the classical cannabinoid prototype HHC-DMH. In HHC-DMH and other biologically active classical cannabinoids in which the ring system deviates only slightly from planarity (~10°–20°), the three cannabinoid pharmacophores (PH, NAH, and SC) align themselves optimally with regard to the respective groups with which they interact at the active site. However, for CP-47,497 and other nonclassical cannabinoids, such an alignment of the three pharmacophores requires an additional amount of energy of at least 2 kcal/mol, a consideration which is reflected in the slightly lower potencies of nonclassical cannabinoids when compared to their structurally equivalent classical cannabinoid analogs.[9]

## Conclusions

With the help of 2D NMR techniques and computer molecular modeling, we have defined the preferred conformation for CP-47,497 which shows that the A- and C-rings are almost perpendicular to each other ($\varphi_1 = 62°$) and the phenolic OH is coplanar with the aromatic ring with its hydrogen pointing away from the cyclohexyl ring ($\varphi_2 = -1.5°$), while the dimethylheptyl side chain randomly adopts one of four equivalent minimum-energy conformers (see Table 3). NMR data show that the conformer having a $\varphi_1$ of 62° appears to be preferred on the NMR time scale, although the A- and C-rings may undergo dynamic time averaging, interconverting between two conformations ($\varphi_1$ = 62 or −116°). However, the single energy-favored conformer does not necessarily represent the conformation at the site of action. A graphic representation comparing the conformations of CP-47,497 and HHC-DMH shows that the lowest energy conformer for CP-47,497 can interact with the cannabinoid receptor active site in a similar manner as the classical cannabinoid prototype HHC-DMH. Such an interaction, however, would require a

minimal energy of 3 kcal/mol in order to obtain an alignment of the phenolic and cyclohexane rings of CP-47,497 in the proper pharmacophoric orientation. It should be pointed out that the preferred conformation of CP-47,497 was experimentally determined in a relatively hydrophobic solvent ($CDCl_3$). Arguably, such an environment may, to a certain extent, approximate the hydrophobic environment of the membrane and the membrane-bound receptors.

**Acknowledgment.** We thank Peter Ziegler (Bruker, Inc.), Susan S. Pochapsky (Bruker, Inc.), Fora Chen (Biosym, Inc.), and Eric M. Billings (University of Connecticut) for their assistance in our research work. This work was supported by grants from the National Institute on Drug Abuse (DA-3801, DA-07215, and DA-00152).

## References

(1) Dewey, W. L. Cannabinoid pharmacology. *Pharmacol. Rev.* **1986**, *38*, 151–178.
(2) Mechoulam, R., Ed. *Cannabinoids as Therapeutic Agents*. CRC Press: Boca Raton, FL, 1986.
(3) Matsuda, L. A.; Lolait, S. J.; Brownstein, M. J.; Young, A. C.; Bonner, T. I. Structure of a cannabinoid receptor and functional expression of the cloned cDNA. *Nature* **1990**, *346*, 561–564.
(4) Makriyannis, A.; Rapaka, R. S. The molecular basis of cannabinoid activity. *Life Sci.* **1990**, *47*, 2173–2184.
(5) (a) Gerard, C. M.; Mollereau, C.; Vassart, G.; Parmentier, M. Nucleotide sequence of a human cannabinoid receptor cDNA. *Nucleic Acids Res.* **1990**, *18*, 7142. (b) Gerard, C. M.; Mollereau, C.; Vassart, G.; Parmentier, M. Molecular cloning of a human cannabinoid receptor which is also expressed in testis. *Biochem. J.* **1991**, *279*, 129–134.
(6) Munro, S.; Thomas, K. L.; Abu-Shaar, M. Molecular characterization of a peripheral receptor for cannabinoids. *Nature* **1993**, *365*, 61–65.
(7) Johnson, M. R.; Melvin, L. S.; Althuis, T. H.; Bindra, J. S.; Harbert, C. A.; Milne, G. M.; Weissman, A. Selective and potent analgesics derived from cannabinoids. *J. Clin. Pharmacol.* **1981**, *21*, 271s–282s.
(8) Melvin, L. S.; Johnson, M. R.; Harbert, C. A.; Milne, G. M.; Weissman, A. A cannabinoid derived prototypical analgesic. *J. Med. Chem.* **1984**, *27*, 67–71.
(9) Johnson, M. R.; Melvin, L. S. The discovery of non-classical cannabinoid analgesics. In *Cannabinoids as Therapeutic Agents;* Mechoulam, R., Ed.; CRC Press: Boca Raton, FL, 1986; pp 121–146.
(10) Bendall, M. R.; Pegg, D. T. Complete accurate editing of decoupled $^{13}C$ spectra using DEPT and a quaternary-only sequence. *J. Magn. Reson.* **1983**, *53*, 272–296.
(11) Rance, M.; Sorensen, O. W.; Bodenhausen, G.; Wagner, G.; Ernst, R. R.; Wuthrich, K. Improved spectral resolution in COSY $^1H$ NMR spectra of proteins via double quantum filtering. *Biochem. Biophys. Res. Commun.* **1983**, *117*, 479–485.
(12) Bax, A.; Morris, G. An inproved method for heteronuclear chemical correlation by two-dimensional NMR *J. Magn. Reson.* **1981**, *42*, 501–505.
(13) Bodenhausen, G.; Kogler, H.; Ernst, R. R. Selection of coherence-transfer pathways in NMR pulse experiments. *J. Magn. Reson.* **1984**, *58*, 370.
(14) Diehl, P.; Kellerhals, H.; Lustig, E. Computer assistance in the analysis of high-resolution NMR spectra. In *NMR: Basic Principles and Progress*; Diehl, P., Fluck, E., Kosfeld, R., Eds.; Springer-Verlag: New York, 1972; pp 1–96.
(15) Kriwacki, R. W.; Makriyannis, A. The conformational analysis of $\Delta^9$- and $\Delta^{9,11}$-tetrahydrocannabinols in solution using high resolution nuclear magnetic resonance spectroscopy. *Mol. Pharmacol.* **1989**, *35*, 495–503.
(16) Biosym InsightII/DISCOVER (version 2.0.0/2.7.0) is a molecular modeling software package of Biosym Technologies Inc., Barnes Canyon Rd., San Diego, CA 92121.
(17) Lautenschlager, P.; Brickmann, J.; Ruiten, J. V.; Meier, R. J. Conformations and rotational barriers of aromatic polyesters. *Macromolecules* **1991**, *24*, 1284–1292.
(18) Hagler, A. T. Theoretical simulation of conformation, energetics, and dynamics of peptides. In *The Peptides: Conformation in Biology and Drug Design*; Hruby, V. J., Udenfriend, S., Meienhofer, J., Eds.; Academic Press, Inc.: New York, 1985; Vol. 7, pp 214–300.
(19) Karplus, M. Vicinal proton coupling in NMR. *J. Am. Chem. Soc.* **1963**, *85*, 2870.
(20) Kessler, H., Bermel, M. Methods in stereochemical analysis. In *Application of NMR Spectroscopy to Problems in Stereochemistry and Conformational Analysis;* Takenchi, Y., Marchand, A. P., Eds.; VCH Press: Dedfield Beach, 1986; pp 179–205.
(21) Hagler, A. T.; Dauber, P.; Osguthorpe, D. J.; Hempel, J. Dynamics and conformational energetics of a peptide hormone: vasopressin. *Science* **1985**, *227*, 1309.
(22) Rosenqvist, E.; Ottersen, T. The crystal and molecular structure of $\Delta^9$-tetrahydrocannabinolic acid B. *Acta Chem. Scand.* **1975**, *B29*, 379–384.
(23) Silverstein, R. M.; Bassler, G. C.; Morrill, T. C. *Spectrometric Identification of Organic Compounds*, 4th ed.; John Wiley & Sons, Inc.: New York, 1981; pp 249–262.
(24) Reggio, P. H.; Greer, K. V.; Cox, S. M. The importance of the orientation of the $C_9$ substituent to cannabinoid activity. *J. Med. Chem.* **1989**, *32*, 1630–1635.
(25) Makriyannis, A. The role of the phenolic hydroxyl group during the tetrahydrocannabinol:membrane interactions. In *Marijuana: An International Research Report:* Chesher, G., Consroe, P., Musty, R., Eds.; Australian Publishing Service: Canberra, 1988; pp 437–451.
(26) Dewar, M. A.; Zoebisch, E. G.; Healy, E. F.; Stewart, J. P. AM1, a new general purpose quantum mechanical molecular mode. *J. Am. Chem. Soc.* **1985**, *107*, 902–3909.
(27) Van der Schyf, C. J.; Mavromoustakos, T.; Makriyannis, A. The conformation of (−) 8$\alpha$ and (−) 8$\beta$-hydroxy-$\Delta^9$-tetrahydrocannabinols and their interactions with model membranes. *Life Sci.* **1988**, *42*, 2231–2239.
(28) Booth, H. Applications of hydrogen nuclear magnetic resonance spectroscopy to the conformational analysis of cyclic compounds. *Prog. NMR Spectrosc.* **1969**, *5*, 149–381.
(29) Reggio, P. H.; Panu, A. M.; Miles, S. Characterization of a region of steric interference at the cannabinoid receptor using the active analog approach. *J. Med. Chem.* **1993**, *36*, 1761–1771.